Mode spectrum of multi-longitudinal mode pumped near-degenerate OPOs with volume Bragg grating output couplers

Markus Henriksson[1,2,*], Lars Sjöqvist[1], Valdas Pasiskevicius[2] and Fredrik Laurell[2]

[1]*Laser Systems Group, FOI - Swedish Defence Research Agency, P.O. Box 1165, 581 11 Linköping, Sweden*
[2]*Laser Physics, KTH - Royal Institute of Technology, 106 91 Stockholm, Sweden*
**mahe@foi.se*

Abstract: Spectral requirements for the first stage OPO used to pump a tandem ZGP mid-infrared OPO are theoretically investigated. Based on these requirements we demonstrate a singly-resonant type-I OPO including periodically poled $KTiOPO_4$ and volume-Bragg gratings as output couplers. Singly resonant oscillation is demonstrated very close to degeneracy, where signal and idler spectra are not well separated. Investigations of the longitudinal mode spectrum and the idler spectrum with high resolution using a scanning Fabry-Perot interferometer show the essential role played by the phase correlations of the multi-longitudinal mode Q-switched pump laser in formation of the nonresonant idler spectrum.

OCIS codes: (190.4970) Parametric oscillators and amplifiers; (050.7330) Volume holographic gratings.

References and links

1. S. Haidar, K. Miyamoto, and H. Ito, "Generation of tunable mid-IR (5.5-9.3 μm) from a 2 μm pumped $ZnGeP_2$ optical parametric oscillator," Opt. Commun. **241**(1–3), 173–178 (2004).
2. K. L. Vodopyanov, O. Levi, P. S. Kuo, T. J. Pinguet, J. S. Harris, M. M. Fejer, B. Gerard, L. Becouarn, and E. Lallier, "Optical parametric oscillation in quasi-phase-matched GaAs," Opt. Lett. **29**(16), 1912–1914 (2004).
3. S. Brosnan, and R. Byer, "Optical Parametric Oscillator Threshold and Linewidth Studies," IEEE J. Quantum Electron. **15**(6), 415–431 (1979).
4. P. Schlup, G. W. Baxter, and I. T. McKinnie, "Single-mode near- and mid-infrared periodically poled lithium niobate optical parametric oscillator," Opt. Commun. **176**(1–3), 267–271 (2000).
5. B. Jacobsson, M. Tiihonen, V. Pasiskevicius, and F. Laurell, "Narrowband bulk Bragg grating optical parametric oscillator," Opt. Lett. **30**(17), 2281–2283 (2005).
6. M. Henriksson, L. Sjoqvist, V. Pasiskevicius, and F. Laurell, "Narrow linewidth 2 μm optical parametric oscillation in periodically poled $LiNbO_3$ with volume Bragg grating outcoupler," Appl. Phys. B **86**(3), 497–501 (2007).
7. M. Henriksson, M. Tiihonen, V. Pasiskevicius, and F. Laurell, "$ZnGeP_2$ Parametric Oscillator Pumped by a Linewidth Narrowed Parametric 2 μm Source," Opt. Lett., **31**(12), 1878–1880 (2006).
8. M. Henriksson, M. Tiihonen, V. Pasiskevicius, and F. Laurell, "Mid-infrared ZGP OPO pumped by near-degenerate narrowband type-I PPKTP parametric oscillator," Appl. Phys. B **88**(1), 37–41 (2007).
9. M. Henriksson, L. Sjoqvist, V. Pasiskevicius, and F. Laurell, "Tandem PPKTP and ZGP OPO for mid-infrared generation," Proc. SPIE **7115**, 71150O (2008).
10. G. Arisholm, G. Rustad, and K. Stenersen, "Importance of pump-beam group velocity for backconversion in optical parametric oscillators," J. Opt. Soc. Am. B **18**(12), 1882–1890 (2001).
11. G. Arisholm, "Quantum noise initiation and macroscopic fluctuations in optical parametric oscillators," J. Opt. Soc. Am. B **16**(1), 117–127 (1999).
12. M. Imai, Y. Ohtsuka, and S. Satoh, "Spatial coherence analysis of light propagation in optical fibers by interferometric methods," J. Opt. Soc. Am. A **3**(7), 1059–1064 (1986).
13. H. Kogelnik, "Coupled wave theory for thick hologram gratings," Bell Syst. Tech. J. **48**, 2909–2947 (1969).
14. G. Anstett, and R. Wallenstein, "Experimental investigation of the spectro-temporal dynamics of the light pulses of Q-switched Nd:YAG lasers and nanosecond optical parametric oscillators," Appl. Phys. B, **79**(7), 827–836 (2004).
15. P. N. Butcher, and D. Cotter, *The elements of nonlinear optics,* (Cambridge, 1990).

#115392 - $15.00 USD Received 6 Aug 2009; revised 7 Sep 2009; accepted 7 Sep 2009; published 16 Sep 2009

1. Introduction

High average power and high-energy coherent radiation in the mid-infrared (MIR) spectral region spanning wavelengths from 3 μm to about 8 μm is desirable for a number of applications including directed countermeasures, remote sensing and surgery. One of the methods of obtaining this radiation is by using a tandem optical parametric oscillator (OPO) system which can be pumped by well established Q-switched lasers at 1064 nm. Typically such tandem OPO consists of a degenerate or near-degenerate OPO operating at 2 μm which in turn pumps a mid-infrared (MIR) OPO employing ZGP or orientation-patterned GaAs [1,2]. The most critical link in this system is the first OPO at 2 μm. In designing the tandem OPO one needs to take into account that the bandwidth of the radiation generated at 2 μm affects the efficiency of the subsequent MIR OPO. This is a well known fact, but to answer exactly how much the total efficiency suffers as the 2 μm radiation bandwidth is increased is not straightforward. This is the first question we set to answer in this work.

Near degeneracy the gain bandwidth in a type I configuration, where signal and idler have the same polarization, can be several hundred nm. This is especially true for quasi-phase matching (QPM) in periodically poled crystals. OPOs near 2 μm have an important application as pump sources for mid-IR OPOs. In early realizations of tandem OPO systems type-II interaction in bulk KTP crystals was used for the first-stage OPO. The use of type-I interaction in QPM crystals can improve the system efficiency considerably due to the higher nonlinearity and walk-off free interaction. It also enables the use of both signal and idler for pumping the MIR OPO. However, spectral narrowing is mandatory for efficient MIR OPO pumping, as shown below. The traditional ways to reduce the bandwidth of an OPO by use of etalons and gratings in the cavity [3,4] are not optimal due to additional losses and limited free-spectral range of etalons. Moreover, an additional intracavity element increases the OPO cavity length which also reduces the efficiency. The use of a volume Bragg grating (VBG) output coupler in an OPO cavity, first demonstrated by Jacobsson *et al.* [5], has been shown to be a more efficient way of narrowing the spectrum of an OPO. We have previously shown narrowband singly-resonant OPO operation near degeneracy with both PPLN and PPKTP crystals [6–9]. Efficient pumping of a ZGP OPO by the combined signal and idler from a periodically poled KTP (PPKTP) OPO with a VBG was also demonstrated [8,9].

Thus after theoretically determining the pump bandwidth limitation in the tandem OPO system, we experimentally investigate the longitudinal mode spectrum of a nearly-degenerate singly-resonant PPKTP OPO (SRO) with VBG output coupler, pumped by a multi-longitudinal mode laser. In particular, we demonstrate that by employing a narrowband VBG the SRO operation can be achieved even when the signal and the idler spectra start overlapping. This allows effective SRO operation in the type-I QPM OPO very close to degeneracy, thus avoiding overconstrained doubly-resonant situation which would result in a highly unstable operation in the OPO without active cavity stabilization. We also show how the temporal coherence of the pump plays a crucial role in formation of the nonresonant idler spectrum.

2. Pump bandwidth limitation in tandem OPO

The acceptance bandwidth of the pump in parametric devices can be estimated from the phase matching condition only when one of the parametric waves has fixed frequency. For instance by assuming a fixed signal wavelength the pump acceptance bandwidth $\Delta\omega_p$ to the first order can be obtained from Eq. (1) (see e.g [10].):

$$\Delta\omega_p < \frac{\pi}{L}\left|\frac{v_{g,p}v_{g,i}}{v_{g,i}-v_{g,p}}\right|, \qquad (1)$$

where L is the length of the nonlinear crystal and $v_{g,p}$, $v_{g,i}$ are the group velocities of the pump and the idler waves, respectively. For a 14 mm long ZGP crystal pumped at 2.128 μm Eq. (1)

#115392 - $15.00 USD Received 6 Aug 2009; revised 7 Sep 2009; accepted 7 Sep 2009; published 16 Sep 2009

gives a maximum pump bandwidth of 275 GHz, or 4.1 nm, for OPA of a single longitudinal mode signal at 3.7 µm.

The situation in a free running OPO, is much more complicated as both signal and idler have finite spectral bandwidths and can adjust their wavelengths to compensate for a small change in the pump wavelength. A simulation model can be used to test the dependence of the OPO conversion efficiency on the pump bandwidth. The simulations were performed with the OPO simulation engine SISYFOS, developed at the Norwegian Defence Research Establishment [11]. As a large number of simulation runs were to be performed with high spectral resolution the simulation was done in plane wave geometry. The 2.128 µm pump spectrum is described by a Lorentz function and the spectral width given here is the FWHM bandwidth. The individual modes in the pump are assigned random complex Gaussian-distributed amplitudes, and the modulation pattern is periodic with a period that is several times shorter than the ZGP OPO roundtrip time with no fractional relation between the roundtrip times. In the simulated example, a ZGP OPO with parameters similar to the ones in earlier experiments by the authors [9], three different pump energies were studied. From Fig. 1 it can be seen that there is both an increase in threshold energy and a decrease in slope efficiency when the pump bandwidth is increased. The simulation results (see Fig. 1) also show that there is no clear limit of the acceptable pump bandwidth but that the conversion efficiency gradually decreases with increasing bandwidth.

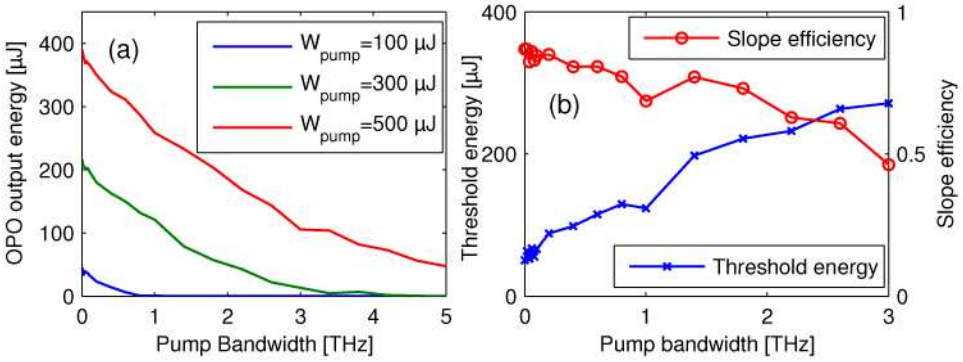

Fig. 1. (a) Simulated ZGP OPO output energy as a function of pump bandwidth for three different pump energies. (b) Simulated OPO threshold energy and slope efficiency as a function of pump bandwidth.

Operation of the first-stage OPO exactly at degeneracy should be avoided due to the doubly-resonant oscillation nature with increasing output fluctuations owing to back-conversion. Without active cavity stabilization and pump retro-reflection, the operation of type-I OPOs at degeneracy result in lower conversion efficiency. With signal and idler separated in frequency but having the same polarization they can still be used for pumping of the same second stage OPO, which is not the case when a type II OPO is used for the first OPO stage. Consequently we simulated the effect of detuning from degeneracy for the first-stage OPO on the output energy of the second-stage ZGP OPO. The pumping spectra used were not realistic OPO spectra but two identical spectra of the same type that were used when simulating the effect of the bandwidth. The results for different pump energies are shown in Fig. 2. If the detuning is not too large, say below 500 GHz (7.5 nm), there is clear evidence that both the signal and idler coherently contribute to the output of the second OPO. This leads to enhancement of the total system efficiency. For larger detuning, the coherent enhancement gradually decreases and the ZGP OPO will generate two independent multimode signal-idler pairs pumped by the signal and idler of the first OPO, respectively. This effect is illustrated in the right part of Fig. 2 where the simulation with 40 GHz (0.6 nm) detuning from degeneracy of the signal in the first OPO gives a single broad peak for the signal and one for the idler of the ZGP OPO while the simulation with 500 GHz (7.6 nm)

#115392 - $15.00 USD Received 6 Aug 2009; revised 7 Sep 2009; accepted 7 Sep 2009; published 16 Sep 2009

detuning in the first OPO gives double peaked signal and idler spectra. The double peaked nature of the spectra has also been observed experimentally [9].

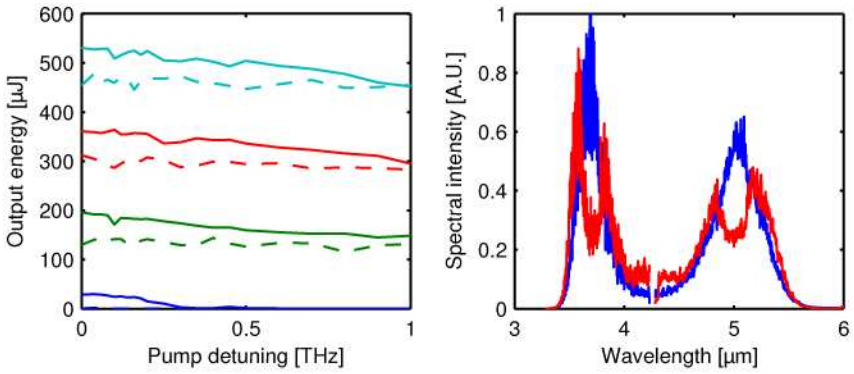

Fig. 2. Left: The calculated output energy of the ZGP OPO pumped by the signal and idler of an OPO with varying detuning from degeneracy. Solid lines are the simulations with both pump components applied simultaneously and dashed lines with the two components simulated separately and the generated energy summed afterwards. The total pump energies were 100, 300, 500 and 700 μJ with half of that energy in each component. Right: Output spectra from two of the simulations where the pump was detuned 40 GHz (blue) and 500 GHz (red) from degeneracy.

3. Experimental setup

The pump laser was a commercial multi-longitudinal mode diode-pumped Q-switched Nd:YVO_4-slab laser, providing a maximum energy of 1.8 mJ in 9 ns-long pulses. For the OPO mode characterization experiments the pump laser was operated at 100 Hz repetition rate in order to avoid increased heat-load and associated spectral shift in the reflectivity of the OPO VBG output coupler. The pump laser spectral width was found to be 28 GHz by measuring interference fringe visibility using an image-rotating Michelson interferometer, where one arm used two mirrors in a corner reflector arrangement while the other arm used a flat mirror on a translator (similar to the arrangement in [12]). An optical isolator was used to decouple the pump laser from the OPO cascade, while the half-wave plate–polarizer combination was used to adjust pump power. The pump beam was loosely focused to a waist ($1/e^2$ intensity radius) of 0.34 × 0.30 mm^2 in the horizontal and vertical directions, respectively.

Two different 1 mm-thick PPKTP crystals having physical lengths of 20 mm and 10 mm (with corresponding lengths of QPM periods of 16 mm and 8 mm, respectively) and QPM periods of 38.85 μm and 38.8 μm, respectively, were used as the OPO gain media. For the longer crystal proper care was taken to prevent parasitic oscillation by AR coating (for pump and signal) and non-parallelism of the crystal optical faces, while the shorter crystal was uncoated. The parametric gain for both crystals was kept at degeneracy by adjusting the PPKTP temperatures (temperatures of 57 °C and 89 °C for QPM periods of 38.85 μm and 38.8 μm, respectively). Different crystal lengths allowed variation of the OPO longitudinal mode separation and to reach operational regimes where the effect of the pump coherence on the idler output spectrum could be easily demonstrated.

We used a simple linear OPO cavity which employed a dichroic incoupling mirror, highly transmitting for the pump and highly reflecting for the signal-idler range. The cavity was completed by one of three available output couplers, namely, a broadband dielectric mirror reflective between 2 μm and 2.4 μm, a VBG1 reflective at 2128.6 nm and a VBG2 reflective at 2122 nm. The VBG reflectivity spectra were 0.5 nm (FWHM) in both cases. All output couplers had a nominal maximum power reflectivity of 50%. The VBG optical surfaces were polished to give a small angle between the surface normal and the grating vector to avoid broadband feedback and then AR-coated for the pump and signal wavelengths. This means

#115392 - $15.00 USD Received 6 Aug 2009; revised 7 Sep 2009; accepted 7 Sep 2009; published 16 Sep 2009

that the cavity was perfectly singly resonant (at least for VBG2) and that there was no pump feedback. In order to obtain resolution in the measurements of individual longitudinal modes, the OPO cavity lengths were kept as small as possibly, ultimately determined by the mechanical constraints.

For lower resolution spectral measurements we employed a grating monochromator with an effective resolution of 0.5 nm. The OPO longitudinal modes were resolved using a scanning plane-mirror Fabry-Perot interferometer with a finesse of 70. The Fabry-Perot mirror separation of 1.5 mm gives a frequency resolution of about 1.4 GHz. During measurement the Fabry-Perot was repeatedly scanned over the range of up to 4 free spectral ranges (FSR) with one data point in the frequency scan corresponding to one OPO pulse. The total length of the scans corresponds to up to 16 000 OPO pulses. The estimated frequency measurement error is about 10% and arises from the accuracy in determining the mirror spacing and the FSR measurement.

4. Experimental results and discussion

The PPKTP OPO output spectra obtained with the three different output couplers are compared in Fig. 3. Here the spectrum was measured with the grating monochromator. In the OPO with the dielectric mirror output coupler the spectrum extends over 14 THz and, by reference to Fig. 1 it can be seen that most of the generated power would be wasted in the cascaded OPO scheme. For the VBG output couplers the OPO spectral widths are limited by the monochromator resolution. Figure 4 shows the signal and idler spectra of the OPO containing the 20 mm-long PPKTP with the VBG2 output coupler (reflective at 2122 nm) as measured by the Fabry-Perot interferometer. The 13 nm separation of signal and idler corresponds to 8.6 times the FSR, so that the different orders of signal and idler were interleaved with each other, but the signal and idler spectra of different orders did not overlap significantly. In the resonant signal spectrum several longitudinal modes are clearly visible with an average mode separation of 3.44 GHz.

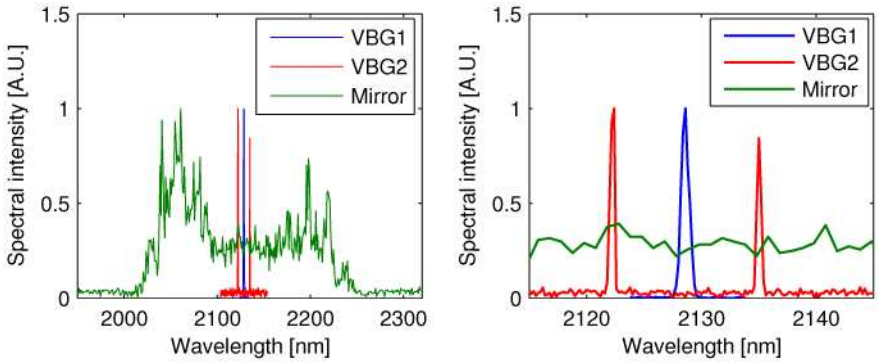

Fig. 3. Output spectra from the OPO using three different output couplers shown at two different wavelength scales.

This mode separation is well in agreement with the theoretical value of 3.45 GHz assuming 7.2 mm optical path in the OPO cavity outside the PPKTP crystal and taking into account the VBG dispersion. Thus the cavity roundtrip time can be expressed as $T_{RT}(\omega) = T_{cav}(\omega) + d\phi/d\omega_{VBG}\big|_{\omega}$. The dispersion of the VBG having a length d, can be readily calculated from the reflectivity phase (Eq. (2)) [13]:

$$\phi = -\arctan\left(\frac{\delta}{\sqrt{\kappa^2-\delta^2}}\tanh\left(\sqrt{\kappa^2-\delta^2}\,d\right)\right), \qquad (2)$$

#115392 - $15.00 USD Received 6 Aug 2009; revised 7 Sep 2009; accepted 7 Sep 2009; published 16 Sep 2009

where the detuning is $\delta = 2\pi n_0 \left(\lambda^{-1} - \lambda_0^{-1} \right)$, the coupling coefficient is $\kappa = \pi n_1 / \lambda$, the Bragg wavelength is $\lambda_0 = \Lambda / 2n_0$ defined by the VBG period Λ, and the index of refraction in the VBG is modulated according to $n = n_0 + n_1 \sin(2\pi z / \Lambda)$. Small variations of the longitudinal mode spacing due to VBG dispersion are below the resolution of the measurement. The nonresonant OPO idler does not contain obvious spectral modulation.

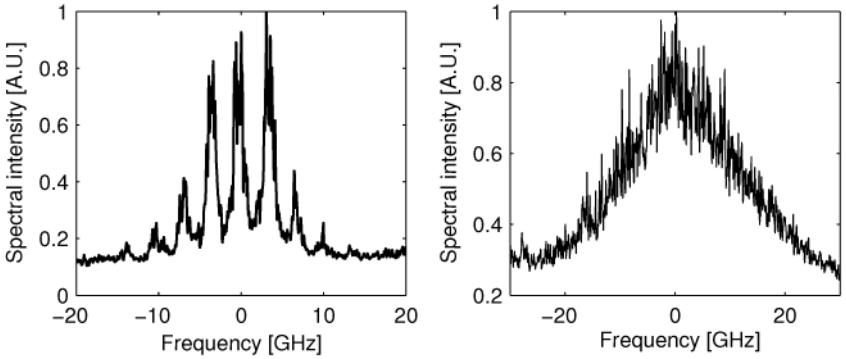

Fig. 4. Spectra of signal (left) and idler (right) with 13 nm (900 GHz) separation measured by Fabry-Perot etalon for maximum pump power

The situation is qualitatively different in the OPO with the same VBG2 output coupler but containing a half as long PPKTP crystal and having approximately half as long OPO cavity. The signal and idler spectra in this OPO are shown in Fig. 5. For this cavity the mode separation is theoretically around 6.25 GHz at the center of the grating and decreases to 6.1 GHz at the first zero in the VBG reflectance spectrum. The measured mode separation is 6.2 GHz in close agreement with the theoretical estimates. This means that the reflectivity variation between adjacent modes is significant and that only a few modes fits within the 33 GHz FWHM reflectance peak of the volume Bragg grating. The signal spectrum contains only three clear longitudinal modes. Obviously single-longitudinal mode operation can be achieved most easily by further reducing the bandwidth of the VBG output coupler. In contrast to the OPO with a longer cavity (see Fig. 4) the idler spectrum in Fig. 5 is modulated with a period corresponding to the signal mode separation in the cavity. The peaks are wider than the measurement resolution and clearly distinguishable. Moreover, we verified that the idler spectrum modulation persists when the OPO cavity length is slightly changed.

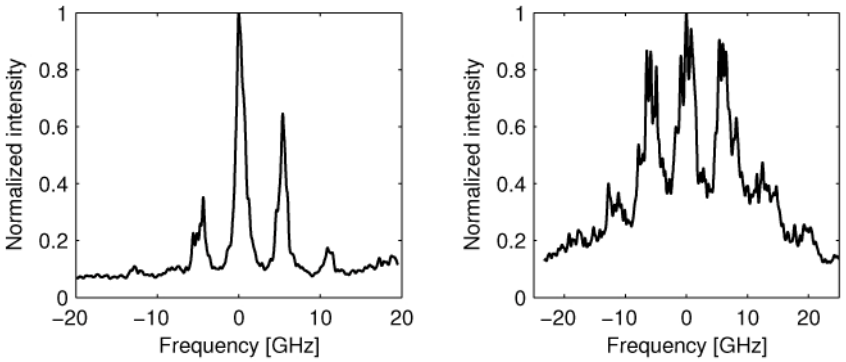

Fig. 5. The signal (left) and idler (right) spectra of the short cavity OPO (10 mm PPKTP crystal) measured by the Fabry-Perot etalon. The signal and idler are separated by 13 nm (900 GHz).

The differences in the idler spectra for the OPO with long and short cavity cannot be attributed to the resolution of the Fabry-Perot interferometer because it was at least two-times

#115392 - $15.00 USD Received 6 Aug 2009; revised 7 Sep 2009; accepted 7 Sep 2009; published 16 Sep 2009

better than the longitudinal modes separation of the longer cavity OPO signal. In order to understand the differences in the idler spectrum we need to take into account coherence properties of the multi-longitudinal mode Q-switched pump pulses. Spectrally resolved streak camera traces in [14] reveal that in an unseeded Q-switched laser adjacent longitudinal mode beating represented by a quasi-period temporal modulation of the intensity envelope are superimposed on apparently random variation of instantaneous spectral intensity maximum over the whole bandwidth of the Q-switched pulse. This behavior can be understood if one considers that there is certain phase correlation among adjacent longitudinal modes comprising the Q-switched pulse spectrum, while the relative phase (and amplitude) variations for the modes separated by more than a correlation radius, specific for each laser, remain largely uncorrelated. In principle this correlation radius could be determined by measuring the RF mode beating spectrum of the pump. Next, we turn to the issue of the idler generated in a single-resonant OPO pumped by such partially coherent pump. The complex polarization dynamics that generates the idler can be expressed as in Eq. (3) [15]:

$$P_i^{(2)}(t) \propto \varepsilon_0 \sum_{n,m} \int_{-\infty}^{\infty} \int_{-\infty}^{\infty} R^{(2)}(\tau_1, \tau_2) E_{p,n}(t-\tau_1) \exp\left[i\phi_{p,n}(t-\tau_1)\right] \times E_{s,m}(t-\tau_2) \exp\left[-i\phi_{s,m}(t-\tau_2)\right] d\tau_1 \, d\tau_2. \quad (3)$$

Here ε_0 is the dielectric constant and $R^{(2)}$ is the second order nonlinear response function, related to the more commonly used susceptibility by the Fourier transform. Causality demands that $R^{(2)}$ is zero for negative τ_1 and τ_2. That the polarization depends on the field at earlier times is due to the mass of the charge carriers in the material, which can also be seen in the frequency dependence of $\chi^{(2)}$. $E_{p,n}$ and $E_{s,m}$ are the real slowly varying amplitudes for pump mode n and signal mode m, respectively, while $\phi_{p,n}(t) = \omega_{p,n} t + \varphi_{p,n}$ and $\phi_{s,m}(t) = \omega_{s,m} t + \varphi_{s,m}$ are the corresponding time dependent phases with $\omega_{p,n}$, $\omega_{s,m}$, $\varphi_{p,n}$ and $\varphi_{s,m}$ being the frequencies and phase offsets of each mode. The idler will contain energy at frequencies $\omega = \omega_{p,n} - \omega_{s,m}$ for all combinations of pump and signal modes, but the amplitude at each frequency depends not only on the mode amplitudes, but also on the phases. Considering that the nanosecond OPO cavity length is normally substantially shorter than that of the pump laser (in our case a pump mode separation of about 1 GHz has been measured), then for each OPO signal mode only the pump modes whose phases are correlated with each other will contribute substantially to the idler generation and thus, to overall OPO efficiency. So for signal mode separation larger than the pump modal phase correlation radius the idler spectrum should contain coherence spikes whose separation corresponds to the signal mode spacing while the width corresponds to the pump modal correlation radius. From Fig. 5 we estimate the pump modal phase correlation radius to be about 3 GHz, corresponding to approximately three correlated modes. On the other hand, when the OPO signal mode separation is reduced to correspond to the pump modal phase correlation radius, the coherence spikes in the idler spectrum disappear as adjacent coherence regions start overlapping.

Finally, it interesting to investigate what happens to the single-resonant OPO spectrum when it is forced to operate as close as possible to degeneracy, i.e. when the VBG central wavelength is detuned from degeneracy point by approximately half of the FWHM bandwidth. This was possible to do with the VBG1 output coupler. The OPO cavity lengths were the same as those in Fig. 4 and Fig. 5. The spectrum of the long-cavity OPO, shown in the left part of Fig. 6, reveals that the OPO is indeed singly resonant, with the longitudinal modes prominent only on the high-frequency signal part of the spectrum. The low-frequency part contains little modulation in agreement with previous discussion. On the other hand, the short-cavity OPO spectrum shows narrow (limited by Fabry-Perot interferometer resolution)

#115392 - $15.00 USD Received 6 Aug 2009; revised 7 Sep 2009; accepted 7 Sep 2009; published 16 Sep 2009

longitudinal modes developed on the high-frequency side of the spectrum and broader coherence spikes on the low-frequency (the idler) side of the spectrum. This is again in agreement with the above explanation of the spectral behavior for a singly-resonant OPO. Furthermore, the OPOs with VBG1 output coupler demonstrate how the superior spectral selectivity of the VBG output couplers allows singly-resonant oscillation to take place even in the case where signal and idler spectra are not well separated.

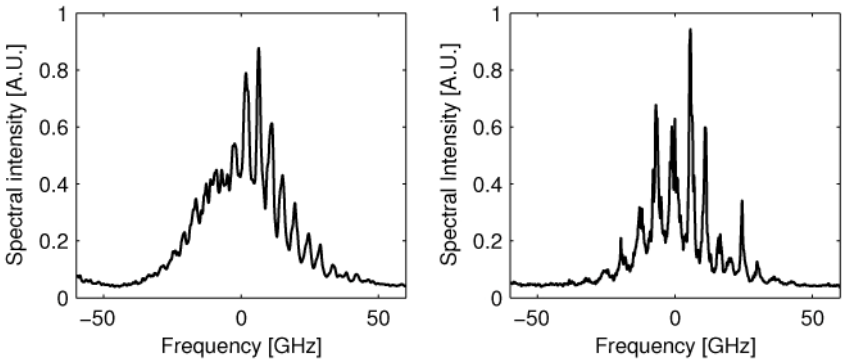

Fig. 6. Fabry-Perot spectra of the OPO close to degeneracy, containing the VBG1 output coupler. Left: the long cavity OPO with the 20 mm PPKTP. Right: the short cavity OPO with the 10 mm PPKTP.

5. Conclusions

We have theoretically determined the spectral requirements of the first stage OPO operating around the degeneracy point at 2.128 μm for efficient pumping of a subsequent tandem ZGP oscillator. These requirements can easily be met in type-I QPM OPOs employing VBG output couplers. The singly-resonant oscillation in this type of device can be maintained even as the signal and idler spectra are not well separated. Investigations revealed that the relative modal phase correlation of the multi-longitudinal mode Q-switched pump laser and signal longitudinal mode separation play a significant role in the spectral shape of the nonresonant idler. It should be stressed that the spectra with VBG output couplers remained stable over the whole pumping range up to 3.5 times above the threshold. Finally, operating the OPO at 20 kHz repetition rate with a cavity containing the 20 mm PPKTP and the VBG2 output coupler we obtained 7.9 W of output radiation with a 30% conversion efficiency. The signal and idler from this configuration have also been used to simultaneously pump a ZGP OPO producing 3.2 W of mid-IR radiation corresponding to a conversion efficiency of 12% from 1.06 μm to the mid-IR [9]. This is one of the highest efficiencies reported from a tandem OPO system.

Acknowledgements

The authors acknowledge valuable discussions about VBG theory with Björn Jacobsson. The 20 mm long crystal was poled by Gustav Strömqvist. This work has been supported in part by the EU FP7 project under grant agreement Nr 224042. We also acknowledge suggestions from one of the reviewers that helped improve the paper.

#115392 - $15.00 USD Received 6 Aug 2009; revised 7 Sep 2009; accepted 7 Sep 2009; published 16 Sep 2009